J. Micromech. Microeng. **9** (1999) 313–318. Printed in the UK PII: S0960-1317(99)00743-3

Effects of a hydrophilic surface in anodic bonding

Duck-Jung Lee†, Byeong-Kwon Ju†, Jin Jang‡, Kwang-Bae Lee§ and Myung-Hwan Oh†

† Electronic Materials and Devices Research Center,
Korea Institute of Science and Technology, PO Box 131, Cheongryang, Seoul 130-650, Korea
‡ Department of Physics, Kyunghee University, Hoigi-dong, Dongdaemun-gu,
Seoul 130-701, Korea
§ Department of Physics, Sangji University, Usan-dong, Wonju 220-702, Korea

E-mail: djlee@kistmail.kist.re.kr

Received 6 January 1999, in final form 27 July 1999

Abstract. This paper presents a study of the anodic bonding technique using a hydrophilic surface. Our method differs from conventional processes in the pre-treatment of the wafer. Hydrophilic surfaces were achieved from dipping in $H_2O/H_2O_2/NH_4OH$ solution. The hydrophilic surface has a large number of –OH groups, which can form hydrogen bonds when two wafers are in contact. This induces a higher electrostatic force, because of the decreasing gap between the glass and silicon wafer. We achieved improved properties, such as a wider bonded area and a higher bond strength than those of conventional methods. Also, the fabricated pressure sensors on the 5-inch silicon wafer were bonded to Pyrex #7740 glass of 3 mm thickness. In order to investigate the migration of the sodium ions, the depth profile at the glass surface by secondary-ion mass spectroscopy and the bonding current were compared with that of conventional methods.

1. Introduction

The bonding technique of two wafers is very important technology in the packaging and design of microstructures [1, 2]. Protection of the device from atmospheric factors is one of the greatest problems for durability and performance [3, 4]. In particular, the anodic bonding method has attracted interest in microsensors and microdevices [5]. The method was invented by Wallis and Pomerantz in 1969 [6]. Anodic bonding can provide a strongly bonded, hermetic seal, which protects the devices from the atmosphere, in spite of the simple process involved [7, 8]. However, a low-temperature bonding is required because wafers with an interconnecting (IC) metal must withstand this temperature without degradation. The internal stress due to the thermal mismatch between the glass and silicon can cause bad effects on the devices' specification. As an example, the induced stress can generate buckling for membranes and resonant beams in micromachine structures [9]. Therefore, the low-temperature process with strong bonding must be adopted to increase the lifetime and durability of the sensors.

In this paper, we have attempted low-temperature bonding with the ability of achieving strong bonds by a hydrophilic surface treatment. The effects of the hydrophilic surface are discussed in terms of the bonded area, bonding strength test, current–time curve and depth profile of the glass surface. The results are compared with those of the non-hydrophilic process.

2. Mechanism

Anodic bonding is typically performed between a sodium-baring glass wafer and a silicon wafer. At elevated temperatures, the mobility of the positive sodium ions presented in the glass is fairly high and the presence of an electric field causes them to migrate to the negatively charged cathode at the back of the glass wafer. As the Na^+ ions migrate towards the cathode, they leave behind a fixed charge in the glass which creates a high electrostatic field with positive charge in the silicon. As a consequence, the surfaces of the contacted wafers are pulled together by the electrostatic force and the atomic bonds Si–O–Si [10] are presumed to occur.

The electrostatic force is generated at the gap between the silicon and glass wafer. When voltage is applied to the wafers, the polarized region in the glass is extended. The voltage across the polarized region, V_p, is given from Poisson's equation [11] as

$$V_p = \frac{\rho X_p^2}{2\varepsilon_G} \quad (1)$$

where ρ is the charge density in the glass, X_p is the thickness of the polarized region and ε_G is the permittivity of the glass. The voltage across the gap, V_g, is given from Laplace's equation [12] as

$$\frac{d^2V}{dX^2} = 0. \quad (2)$$

V depends only on the distance, X, and can be obtained from equation (2) by integrating twice. The two integration

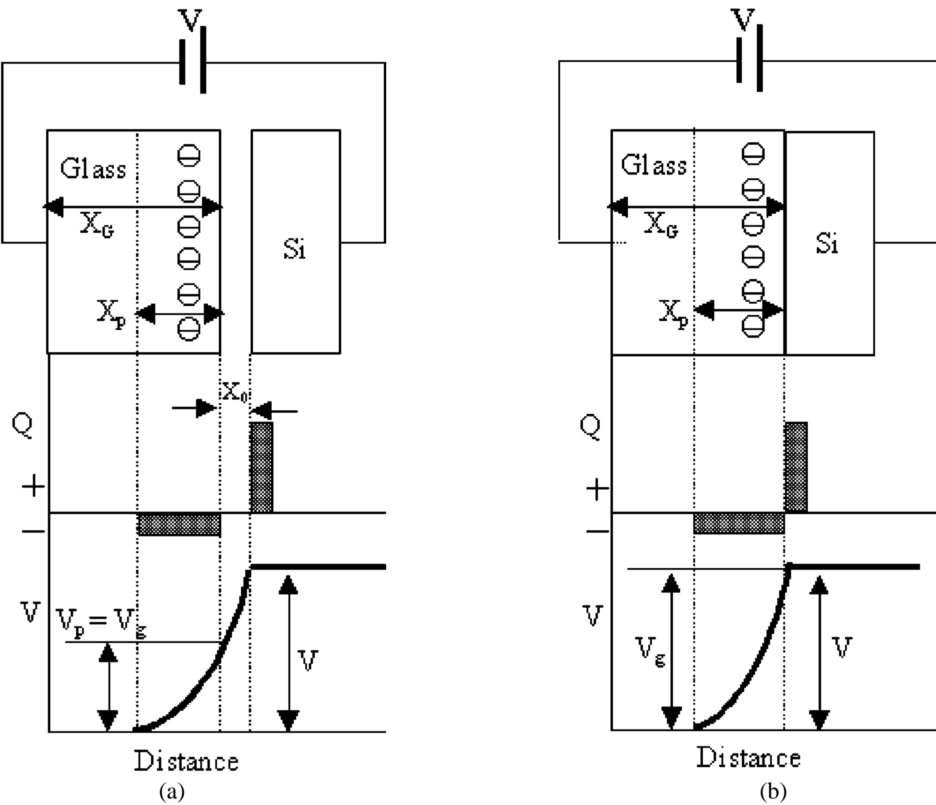

Figure 1. Quantitative presentation of the charge and the potential distribution for (a) group A and (b) group B.

constants are determined from the boundary conditions at $X = 0$, $V = +V$ in the silicon surface and at $X = X_0$, $V = V_p$ in the glass surface, shown in figure 1(a), where positive V is the applied voltage at the silicon wafer and V_p is the potential at the glass surface:

$$V(X) = V_g = \left(\frac{V_p - V}{X_0}\right) X + V. \tag{3}$$

The potential V_g depends on the distance and the applied voltage. If the gap decreases between $0 \leqslant X \leqslant X_0$ in the constant potential, V_g will be increased as a function of distance. The charge and voltage across the silicon–glass structure are shown in figure 1. Figure 1(a) shows that the voltage across the polarized V_p is the same as V_g in the case of a non-hydrophilic surface and figure 1(b) shows that V_g is the same as V in the case of a hydrophilic surface. In figure 1, we can show that the greater decrease of the gap induced a higher potential in the glass wafer. The electrostatic force P for the polarized region is given as [13]

$$\begin{aligned} P &= \frac{1}{2}\varepsilon_0 E_{gap}^2 = \frac{\varepsilon_0}{2X_0^2}(V_g^2) \\ &= \frac{\varepsilon_0}{2X_0^2}\left[\left(\frac{V_p - V}{X_0}\right) X + V\right]^2. \end{aligned} \tag{4}$$

From equation (4), the electrostatic force depends on the voltage of the polarized region, V_p, applied voltage, V, and the gap, X_0. By using the hydrophilic process, we can cause the surface to have a large number of –OH groups, which results in the formation of more hydrogen bonds when two wafers are contacted. The interface gap between glasses and silicon wafers is reduced in figure 2, where X_{og} is the interface gap in the case of a non-hydrophilic surface and X_{oh} is that in the case of a hydrophilic surface. The gap X_{oh} is decreased and eliminated due to the initial hydrogen bond, which can be observed during the experiment. However, the potential V_p and the electrostatic force P of the hydrophilic surface were higher than that of the non-hydrophilic surfaces as mentioned in equations (1)–(4) and figures 1 and 2. At the elevated temperature, the –OH groups between the silicon and glass wafers start to dehydrate and are replaced by Si–O–Si–O bonds [11].

3. Experimental details

The materials used in the bonding experiments were n-type silicon wafers, which were 200 μm in thickness, 1–10 Ω cm in resistance, 1 inch in diameter and (100)-oriented, and Pyrex #7740 glass wafers, which were 500 μm in thickness and 1 inch in diameter. The glass/silicon bonding was carried out by two types of procedure. Those belonging to group A were bonded using only an anodic bonding process at temperatures in the range 200–300 °C and at voltages in the range 60–300 V_{dc}. Group B were initially contacted through the hydrophilic process followed by the anodic bonding process. In group B, silicon and Pyrex #7740 glass wafers were dipped in $H_2O/H_2O_2/NH_4OH$ (6:1:4) solution at 55–65 °C for 5 min to form the hydrophilic surface. The wafers were dried and assembly contacted afterwards. Then the wafers were partly bonded in the centre or edge, which can be easily observed during the experiment, as shown in figure 3. The glass/silicon assembly was heated on a hot plate and a dc voltage applied to the initial bonded pairs. A positive

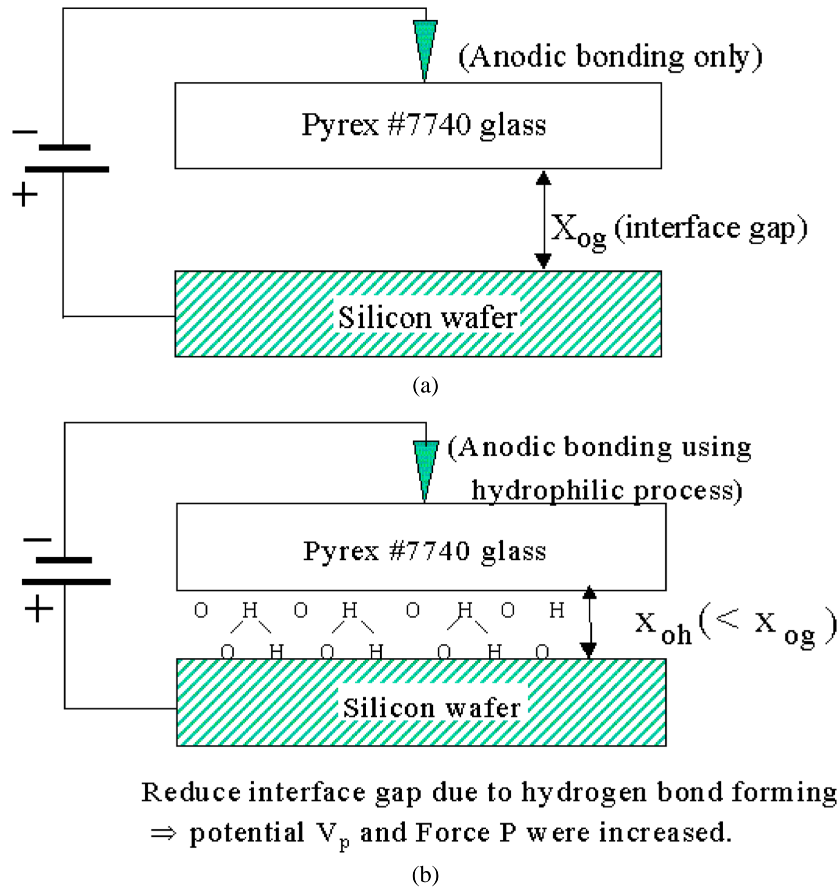

Figure 2. Schematic diagram of the anodic bonding process only (a) and that using the hydrophilic process (b).

electrode was attached to the silicon wafer and an negative electrode was attached to the glass wafer.

The bonded areas and the tensile strengths of bonded specimens were investigated as a function of bonding temperature and applied voltage. The current–time curves were measured by a KEITHLEY 237 meter during the process. The impurity concentrations in the bonded glass were compared with those in a bare glass substrate by secondary ion mass spectroscopy (SIMS).

4. Results and discussion

The bonded area was observed under the illumination of visual light. In order to investigate the effect of voltage and temperature, the glass/silicon wafers were bonded at 300 °C as a function of the applied voltage (table 1(a)) and at 300 V_{dc} as a function of the temperature (table 1(b)). Table 1 shows that the bonded area increased with increasing voltage and temperature. The typical features of the samples belonging to group A and group B are shown in figure 3. The bonding was carried out at 270 °C with an applied voltage of 300 V_{dc}. The bonded area is represented by dark grey and the non-bonded area is represented by a fringe at the wafer edge. We can show the initial bonded area from group A. The hydrogen bonding was caused by the Van der Waals force. Therefore, the reduction of X_0 results in an increase in the electrostatic force, and thus, we get the strong bond and wide bonded area. Figure 4 shows the pressure sensors mounted on Pyrex #7740 glass of 3 mm thickness at 300 °C, 300 V_{dc}.

Table 1. Comparison of the bonded area as a function of bias with temperature = 300 °C (a) and temperature with applied bias = 300 V_{dc} (b). Values are in % (=(Bonded area/Whole wafer area) × 100).

(a)

	Applied bias (V_{dc})						
	60	80	100	150	200	250	300
Group A (Non-hydrophilic)	14	19	25	34	63	83	93
Group B (Hydrophilic)	21	30	52	67	72	96	99

(b)

	Temperature (°C)						
	200	250	260	270	280	290	300
Group A (Non-hydrophilic)	10	15	18	25	47	83	91
Group B (Hydrophilic)	13	47	53	68	82	92	99

Generally, the bonding temperature of the pressure sensors was reported to be less than 450 °C [14]. Our method can mount the pressure sensor of 5 inches in diameter at 300 °C, which is lower than the reported temperature. The silicon pressure sensors are fabricated using a standard IC process on a 5 inch silicon wafer. Subsequently, small cavities were formed on the rearside by an anisotropic etching process.

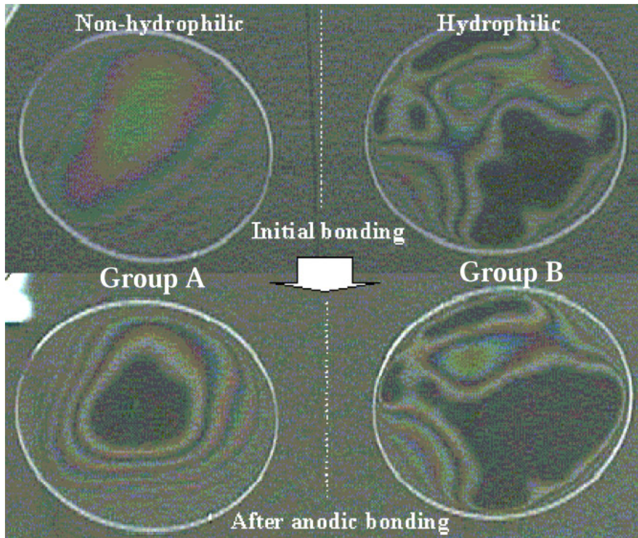

Figure 3. Comparison of the bonded area for and after anodic bonding in group A and group B.

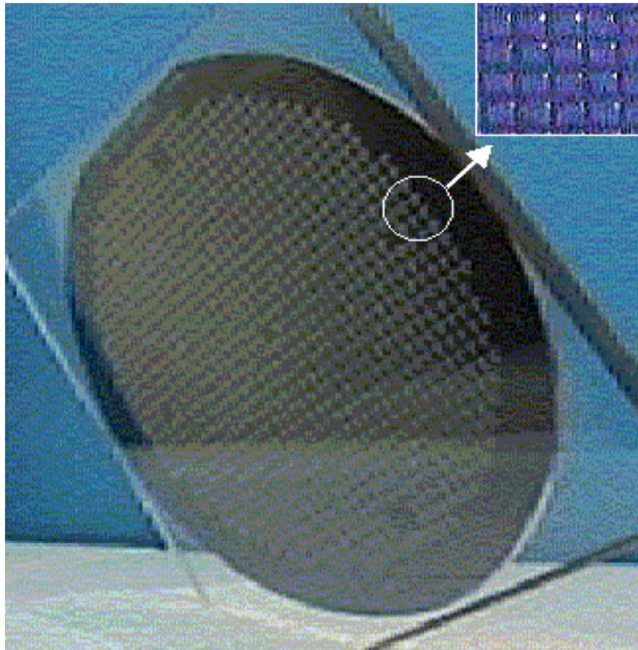

Figure 4. Photograph of the mounted 5 inch pressure sensor on Pyrex #7740 glass with a thickness of 3 mm.

Measurement of the current during the bonding process gives important information about migration of sodium ions. The initial current peak corresponds to the initial transport of sodium ions from the glass to the cathode. The current–time characteristics were measured for group A and group B at 300 °C with an applied voltage of 250 V_{dc} for 10 min. The bonding current decayed rapidly after a few seconds and then remained at a minimum level, as shown in figure 5. The current density profile obtained was well matched with a typical current–time relationship in the anodic bonding process. However, we can show that the currents of group B were higher than those of group A. We infer that initial bonding by the hydrophilic process reduced the gap between the silicon and glass wafers, resulting in higher electric field and a higher migration rate of the sodium ions.

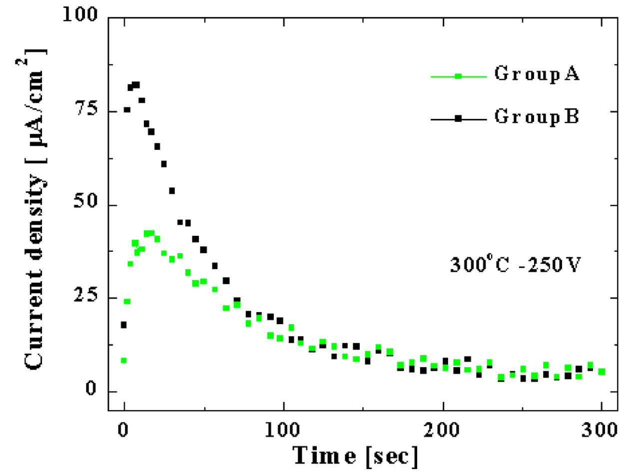

Figure 5. Current–time characteristics during the bonding process.

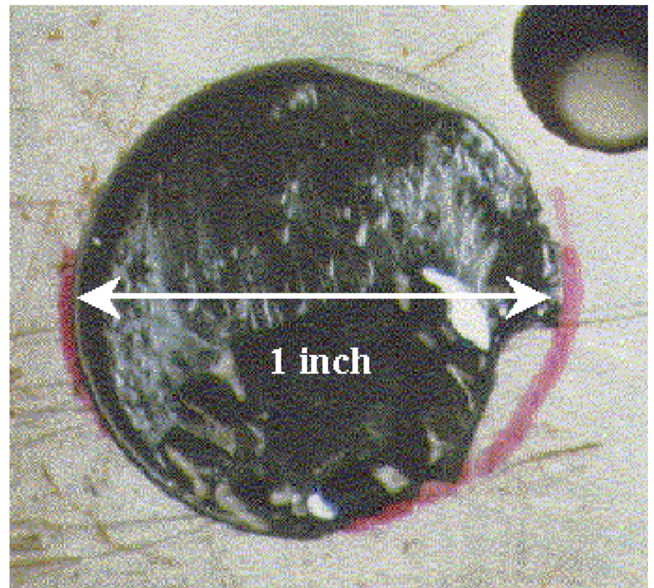

Figure 6. Photograph of fractured glass by tensile test.

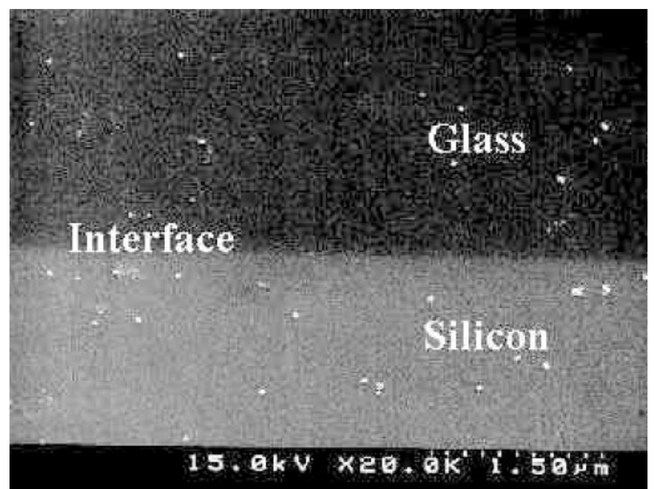

Figure 7. SEM micrographs of the bonded interface region.

In order to determine the bond strength of the glass/silicon wafer pairs, the tensile strength method was

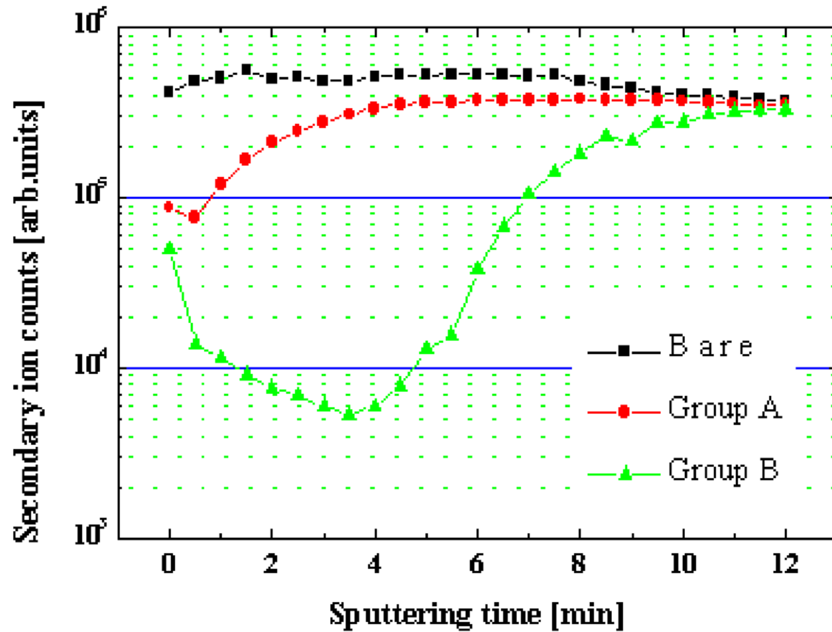

Figure 8. Relative depth profiles of Na for the surface region of glass wafers after de-bonding.

Table 2. Bond strength characteristics as a function of bias with temperature = 300 °C (a) and temperature with applied bias = 300 V_{dc} (b). Values are in MPa.

(a)

	Applied bias (V_{dc})						
	60	80	100	150	200	250	300
Group A (Non-hydrophilic)	2.6	3.2	4.9	7.9	16		
Group B (Hydrophilic)	5.8	9.6	12				

□, fractured glass wafer by tensile test.

(b)

	Temperature (°C)						
	200	250	260	270	280	290	300
Group A (Non-hydrophilic)	X	4.5	10	12.7	15.5		
Group B (Hydrophilic)	6.6	17					

X, not bonding.

employed. The results obtained are illustrated in table 2. The bonding strength is measured as a function of applied voltage at a temperature of 300 °C (table 2(a)) and as a function of temperature at the applied voltage of 300 V_{dc} (table 2(b)). The measured strength was between 0.1 and 20 MPa, and group B has a higher strength than group A under the same conditions. The strength increases with increasing temperature and voltage. If the strength reaches 20 MPa, the measurement limit, all specimens were fractured in the bonded glass wafer. The bulk strength of the Pyrex glass was reported as being lower than 25 MPa [15]. Figure 6 shows the fractured glass by tensile test. Figure 7 shows a SEM micrograph of the cross sectional view of the bonded interface, which is very smooth. The sample was sliced by a diamond cutter and polished by a grinder. The white spots were alumina powder. The sodium ion plays a very important role in anodic bonding. A depletion region of sodium ions results in an electrostatic force that pulls ions together and leads to the formation of atomic bonds. In order to investigate the migration of sodium ions during the bonding process, SIMS analysis was carried out on the surface of glass wafers, which were bonded at 300 °C and 250 V_{dc}. The wafer pairs were de-bonded by inserting a blade into the bonded interface. The SIMS data obtained from the surface of a bare glass wafer with a sputtering rate of 100 Å min^{-1} were compared with those for the surfaces of group A and group B glass wafers. Figure 8 shows the relative depth profile of a glass wafer before and after bonding. It is apparent that the sodium ions were depleted in the surface region of the glass wafer near the silicon wafer to be bonded. In the case of group B, we can clearly observe that the depletion region of sodium ions is deeper than that of group A. It is well known that a deeper depletion region results in a stronger bonding strength. Therefore, we propose that the deeper depletion region of group B results in a higher efficiency than group A.

5. Conclusion

In this paper, we have achieved improved properties from a hydrophilic surface process, such as higher strength, wider bonded area, higher current and deeper depletion of sodium ions, under the same conditions. The hydrophilic process generated a large number of –OH groups on the wafer surface and formed hydrogen bonds when wafers were in contact. The hydrogen bonds can decrease the distance of the interface gap, X_0, between the glass and silicon wafers. They induce a higher potential and electrostatic force than in the conventional method. From our method, we bonded the 5 inch silicon-wafer-based pressure sensors to Pyrex #7740 glass with of thickness 3 mm at 300 °C. This method can reduce the thermal residual stress and mechanical strength in the structure by having a low bonding temperature. Therefore, it can be applied to, for example, the mounting and sealing of microelectronic-mechanical systems.

Acknowledgments

This research was supported by the Ministry of Science and Technology and the Ministry of Industry and Energy under the Micromachining Technology Development Program.

References

[1] Fung C D, Cheung P W, Ko W H and Fleming D G 1985 *Micromachining and Micropackaging of Transducers* (Amsterdam: Elsevier Science) p 41
[2] Ju B K 1995 Study on the direct bonding of silicon wafers for microelectromechanical systems *Dr Thesis* The University of Korea, Seoul, p 8
[3] Holloway P H, Sebastain J, Trottier T, Swartand H and Petersen R O 1995 *Solid State Technol.* August 47
[4] Ljibisa Ristic 1994 *Sensors Technol. Devices* 207
[5] Puers B and Lapadatu D 1994 *Sensors Actuators* A **41/42** 129
[6] Wallis G and Pomerantz D I 1969 *J. Appl. Phys.* **40** 3946
[7] Puers B, Peeters E, Bossche V D and Sansen W 1990 *Sensors Actuators* A **21/23** 8
[8] Shimbo M, Furukawa K, Fukuda K and Tanzawa K 1986 *J. Appl. Phys.* **60** 2987
[9] Cozma A and Puers B 1995 *J. Micromech. Microeng.* **5** 98
[10] Yozo Kanda *et al* 1990 *Sensors Actuators* A **21/23** 939
[11] Esashi M and Nakano A 1990 *Sensors Actuators* A **21/23** 931
[12] Cheng D K 1994 *Fundamentals of Engineering Electromagnetics* (Addison-Wesley) p 128
[13] Anthony T R 1983 *J. Appl. Phys.* **54** 2419
[14] Schmidt M A 1998 *IEEE Proc.* **86** 1575
[15] Cozma A and Puers B 1994 *Micromechanics Europe 1994, Workshop Dig.* p 40